J|A|C|S
COMMUNICATIONS

Published on Web 11/28/2002

Dynamics and Fluidity of Amyloid Fibrils: A Model of Fibrous Protein Aggregates

Ami S. Lakdawala,[†] David M. Morgan,[‡] Dennis C. Liotta,[†] David G. Lynn,*[,‡] and James P. Snyder*[,†]

Center for the Analysis of Supramolecular Self-assemblies, Department of Chemistry, Departments of Chemistry and Biology, Emory University, 1521 Pierce Drive, Atlanta, Georgia 30322

Received June 17, 2002

An experimentally defined model for the fibril formed from the core residues of the β-amyloid (Aβ) peptides of Alzheimer's disease, ^{10}YEVHHQKLVFFAEDVGSNKGAIIGLM, Aβ(10−35), has been proposed (Figure 1a).[1] This highly ordered structure consists of in-register parallel β-strands organized in sheets propagating along the fibril axis. Six such sheets laminated with a 10 Å spacing define the dimensions of the rectangular fibril, 60 Å × 80 Å (Figure 1a). Transmission electron microscopy has been used to obtain the fibril periodicity of ∼1200 Å, corresponding to an axial off-set of 1.5° for each peptide. While spectroscopic and scattering analyses report on the average structure, benefiting immensely from the homogeneous assembly of Aβ(10−35), the energetic constraints that contribute to fibril dynamics and stability remain poorly understood. Here we exploit molecular dynamics simulations to extend the structural assignment by providing evidence for a dynamic average ensemble with transient backbone H-bonds and internal solvation contributing to the inherent stability of amyloid fibrils.

Several critical differences exist between the reported fibril structure and known globular proteins,[2] the most notable being the β-sheets of the amyloid model. For example, β-helices closely resemble the planar parallel β-sheets of the amyloid. However, most stretches of β-sheet in native proteins extend for no more than six or seven residues, while the strands in Aβ(10−35) are 26 residues long. To estimate the cost of lengthening a pleated β-conformation, fragments of two, three, four, five, and six residues of the hydrophobic core ^{16}KLVFFA sequence of Aβ(10−35) were modeled. The strands were first constrained to the ideal pleated β-sheet geometry and optimized with the AMBER*/GBSA/H_2O force field.[3] The constraints were then removed, and the systems were reoptimized. The AMBER*/GBSA/H_2O and density functional fixed-point B3LYP/6-31G** energy differences are approximately linear with chain length, favoring the unconstrained peptide by approximately 2 kcal/mol per residue (Supporting Information (SI)).

To understand how the cost of an extended sheet might be accommodated within the fibril, a 6 × 6 block of the structure (Figure 1a, yellow) was constructed in Sybyl 6.7.[4] The starting assembly aligns all backbone amides within each parallel plane at positions constrained initially to the interatomic carbonyl−carbonyl distances established by NMR.[1,5] The peptides were modeled at their isoelectric point, in the absence of salt or counterions, and solvated with TIP waters to provide a 15 Å fluid shell around the assembly. MD simulations with the Kollman all-atom force field under periodic boundary conditions (NTP, Sybyl6.7) were run initially at 20 K and then increased stepwise to 50 and 100 K without constraints.

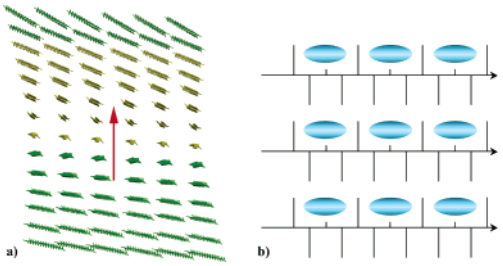

Figure 1. (a) Model of the Aβ(10−35) fibril. Parallel in-register β-strands, oriented perpendicular to and twisting along the propagation axis (red arrow), are arrayed in six parallel sheets. The yellow block represents that segment investigated by MD. (b) Glycine vent. As viewed along the fibril axis, the glycine residues, denoted by the short vertical lines and arrayed on one face of each β-strand, open channels (blue ovals) from ^{24}V to ^{35}M.

Consistent with the solid-state NMR measurements,[1,5] distortions from the β-structure appeared greatest along residues at the C terminus. Glycine residues, distributed i, $i + 4$ along the last 10 positions, opened a channel along the same face of each β-sheet (Figure 1b) to allow water molecules to penetrate and solvate the β-strands. Such "glycine vents" provide access for water to move internally along the entire length of the fibril.

A characteristic and striking feature of the simulation is that only 20−25% of the possible backbone H-bonds, defined as a CO- -HN distance of 1.8−2.3 Å, are present at any point in time. While blocks of H-bonds are present, regions where more than a few H-bonds appear consecutively along the backbone are rare (Figure 2a and SI). Moreover, while the location of the backbone H-bonds vary in time, the total number remains constant. Table 1 illustrates both the constant total number of H-bonds within a 10-ps window across the fibril, as well as highlighting what appears to be a compensating variance of the number of H-bonds in neighboring or adjacent sheets over the same time frame.

A significant number of residues twist out of the hydrogen bonding plane for interaction with nearby solvent molecules, consistent with the calculations above that strand energies limit the number of residues in sequential H-bond registry. The solvent therefore serves both to fill spaces between the sheets, as in the glycine vents, and to shield and stabilize polar backbone and side chain sites within the fiber.

The amino acid side chains that occupy the regions of lamination between the sheets are probably the most dynamic and flexible part of the structure. The motions of the α-carbon positions clearly affect the ability of the amides to be maintained within the H-bonding plane of the sheet as seen in Figure 2b. To evaluate whether these motions may be correlated from sheet to sheet, the number of backbone H-bonds within the middle four sheets was monitored

* Authors for correspondence. E-mail: snyder@euch4e.chem.emory.edu; dlynn2@emory.edu.
[†] Department of Chemistry.
[‡] Departments of Chemistry and Biology.

10.1021/ja0273290 CCC: $22.00

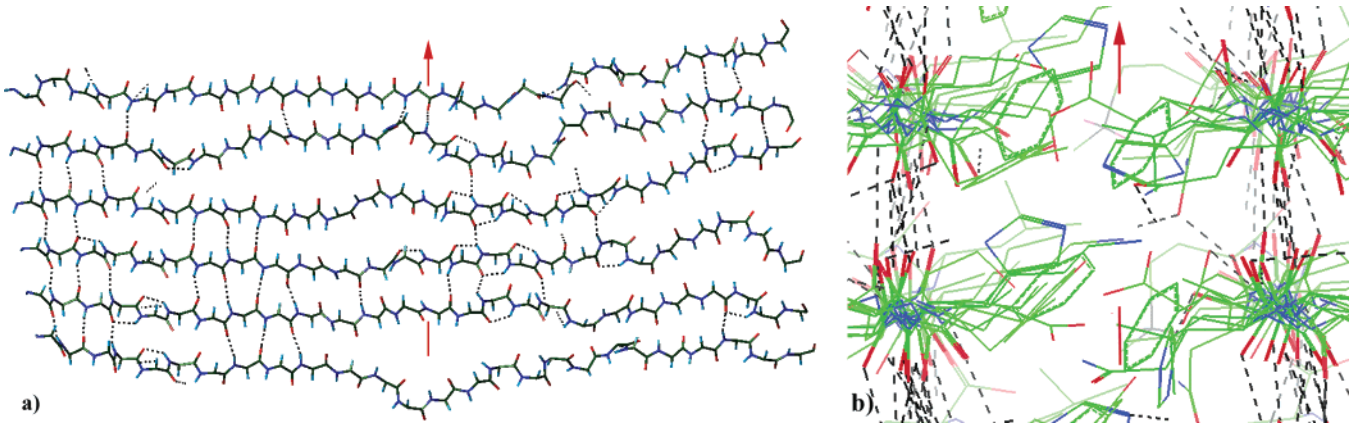

Figure 2. (a) Interior β-sheet after 65 ps of MD at 300 K. Black dashed lines represent H-bonds. Neither side chains nor water molecules are shown. (b) Approximately parallel H-bonding planes as viewed down adjacent β-sheets. Rotation of (a) by 90° about the propagation axis (red arrow) gives the side view as shown in (b) for two parallel laminate sheets. Variable locations of H-bonds (black lines) and side chains are illustrated for the two sheets.

Table 1. Variation of the Number of Backbone H-Bonds (1.8−2.3 Å) within the Four Inner Sheets over 10 ps

	time (picoseconds)											
sheet	55	56	57	58	59	60	61	62	63	64	65	avg
2	32	37	33	37	36	35	37	39	38	34	39	36
3	26	24	30	26	33	24	28	25	24	29	35	28
4	38	31	32	32	39	42	43	35	34	33	35	36
5	28	20	28	30	24	25	29	30	27	30	28	27
total	124	112	123	125	132	126	137	129	123	126	137	127

every 0.5 ps over a 25-ps time frame. Indeed, a weak but statistically significant anticorrelation of motion between adjacent sheets was observed.[6] The array of coupled motions offers an explanation for how the total number of H-bonds predicted within the fibril remains constant (Table 1) even though their positions change over time (SI).

In summary, local networks of backbone H-bonds within the sheets are predicted to be neither extensive nor long-lived (Figure 2a and SI), and fluctuations from ideal β-sheet geometry can be large. Consistent with this prediction, the experimental CO−CO distances measured by ssNMR, particularly within the glycine vents, are markedly greater (approaching 1 Å) than expected for parallel sheets. Within this region, significantly increased backbone mobility is suggested by both larger T_2^{DQ} values and dampening of the DRAWS oscillations at long mixture times. These greater fluctuations near the C terminus could contribute to the larger measured distances; the magnitude of which was found to be dependent on both pH and hydration of the fibril.[5b]

The side chains, disposed nearly perpendicular to the sheets (Figure 2b), dictate laminar stability.[7] Analysis of cross-sheet side-chain contacts in the simulation reveals numerous direct and water-mediated H-bonding interactions that shield normally repulsive polar and charged side-chain juxtapositions. These stabilizing interactions are matched by equally numerous hydrophobic contacts.[8] Therefore, very much unlike globular proteins, the fibril interior adopts an indefinite ensemble average with more "micellar" or "molten-globule-like" properties. Complementary forces *within* and *between* the extended sheets provide both the resilience and stability characteristic of amyloid. The movement of local H-bond patches stabilize the fibril, especially when fortified by long-range backbone electrostatic interactions,[9] but allow for fibril flexibility.[1,5a−d,10] We believe this internal disorder within the fibril contributes to the lowering of the entropic penalty of fibril formation, while explaining the morphological appearance of a flexible, twisting fibril able to form higher order multifibril assemblies. Further experiments are required to quantitatively evaluate fibril hydration and dynamics, but these insights already suggest unique strategies for both general fibril synthesis and the intervention of fibril self-assembly in amyloid disease states.

Acknowledgment. We thank Professor James Kindt for advice on statistical sampling and Grant No. 99-8327 (D.G.L.) from The Packard Foundation Program for financial support.

Supporting Information Available: Energy calculations (PDF) and MD movies. This material is available free of charge via the Internet at http://pubs.acs.org

References

(1) Burkoth, T. S.; Benzinger, T. L. S.; Urban, V.; Morgan, D. M.; Gregory, D. M.; Thiyagarajan, P.; Botto, R. E.; Meredith, S. C.; Lynn, D. G. *J. Am. Chem. Soc.* **2000**, *22*, 7883−7889.
(2) Lolis, E.; Alber, T.; Davenport, R. C.; Rose, D.; Hartman, F. C.; Petsko, G. A. *Biochemistry* **1990**, *29*, 6609.
(3) MacroModel 6.5; cf. http://www.schrodinger.com.
(4) Sybyl 6.7; cf. http://www.tripos.com.
(5) (a) Benzinger, T. L. S.; Gregory, D. M.; Burkoth, T. S.; Miller-Auer, H.; Lynn, D. G.; Botto, R. E.; Meredith, S. C. *Proc. Natl. Acad. Sci. U.S.A.* **1998**, *95*, 13407−13412. (b) Gregory, D. M.; Benzinger, T. L. S.; Burkoth, T. S.; Miller-Auer, H.; Lynn, D. G.; Meredith, S. C.; Botto, R. E. *Solid State Nucl. Magn. Reson.* **1998**, *13*, 149−166. (c) Benzinger, T. L. S.; Gregory, D. M.; Burkoth, T. S.; Miller-Auer, H.; Lynn, D. G.; Botto, G.; Meredith, S. C. *Biochemistry* **2000**, *39*, 3491−3499. (d) Lynn, D. G.; Meredith, S. C. *J. Struct. Biol.* **2000**, *130*, 153−173. (e) Antzutkin, O. N.; Balbach, J. J.; Leapman, D.; Rizzo, N. W.; Reed J.; Tycko R. *Proc. Natl. Acad. Sci. U.S.A.* **2000**, *97*, 13045−13050.
(6) Pearson's Correlation Coefficient (r) was calculated by the number of peptide backbone H-bonds in each interior β-sheet for each 0.5 ps over 25 ps of simulation time, generating 51 data points per β-sheet. $r > 0$ signifies a positive linear correlation, while $r < 0$ is an anticorrelation. A statistically significant correlation has $|r| > 1/n^{1/2} = 1/51^{1/2}$, in this case. Compare Anderson, Robert L. *Practical Statistics for Analytical Chemists*; Van Nostrand Reinhold Company: New York, 1987; pp 118−120.
(7) Sharman, G. J.; Searle, M. S. *J. Am. Chem. Soc.* **1998**, *120*, 5291−5300.
(8) (a) Wiley, A.; Rich, D. H. *Med. Res. Rev.* **1993**, *3*, 327−384. (b) Rich, D. H. In *Perspectives in Medicinal Chemistry*; Testa, B., Kyburz, E., Fuhrer, W., Giger, W., Eds.; VCH: New York, 1993; pp 15−25.
(9) (a) Zhao, Y.-L.; Wu, Y.-D. *J. Am. Chem. Soc.* **2002**, *124*, 1570−1571. (b) Maccallum, P. H.; Poet, R.; Milner-White, E. J. *J. Mol. Biol.* **1995**, *248*, 374−384.
(10) Morgan, D. M.; Lynn, D. G.; Lakdawala, A. S.; Snyder, J. P.; Liotta, D. C. *J. Chin. Chem. Soc.* **2002**, *49*, 459−466.

JA0273290